Near-field optical microscopy of two-dimensional photonic and plasmonic crystals

Igor I. Smolyaninov, Walid Atia, and Christopher C. Davis
Electrical Engineering Department, University of Maryland, College Park, Maryland 20740
(Received 10 June 1998)

Near-field optical images of electromagnetic mode structures in two-dimensional photonic and plasmonic crystals are presented. Interference patterns of plasmon Bloch waves in a plasmonic crystal have been observed. Fourier analysis of the photonic crystal images allows the reconstruction of the refractive index spatial distribution in the crystal. A similar procedure performed on images of a plasmonic crystal allows the recovery of parameters of the surface plasmon interaction with the periodic grooves that constitute the plasmonic crystal structure. [S0163-1829(99)13203-X]

INTRODUCTION

The optical properties of spatially periodic dielectric structures called photonic crystals have attracted much recent interest.[1] The analogy between electromagnetic wave propagation in multidimensionally periodic structures and electron wave propagation in real crystals has proven to be a valuable one. Electron waves traveling in the periodic potential of a crystal are arranged into energy bands separated by gaps in which propagating states are prohibited. Analogous band gaps exist when electromagnetic waves propagate in a periodic dielectric structure with a period comparable to the wavelength. These frequency gaps are referred to as ''photonic band gaps.'' A demonstration of band structure effects in photonic crystals was in the microwave regime.[2] Recently, these effects have been measured in the near-infrared and visible regions.[3] Photonic crystals can have a profound impact in many areas of pure and applied physics. For example, inside a photonic band gap, optical modes, spontaneous emission, and zero point fluctuations are all absent.[1] From a practical point of view photonic crystals can be designed to transmit or reflect light within a specific range of frequencies, and their properties may be tunable by modification of their periodicity or refraction index.

Until recently photonic crystals have been studied by measuring their bulk optical properties. With the invention of the near-field scanning optical microscope[4] (NSOM) local microscopic properties of photonic crystals become accessible to experimental measurement. An application of NSOM techniques to characterize the local density of photon states and the electromagnetic mode structure of a two-dimensional photonic crystal has been reported in Ref. 5. In this work a photonic crystal was locally excited by light leaving a subwavelength aperture at the end of a metal-coated fiber tip. The light transmitted by the crystal was collected in the far field with a microscope objective. The numerical aperture (NA) of the objective was varied. Depending on the value of the NA, the transmitted light with different spatial momenta was integrated and recorded as a function of the position of the fiber tip. The contrast in the images obtained depended strongly on the region in the photon momentum space probed.

Theoretically this situation can be understood as follows: the photonic crystal was excited by a photon source that may be idealized as a δ function in coordinate space. The transmitted light was analyzed as a function of the absolute value of its momentum and the spatial position of the light source. A complicated theoretical model has to be used in order to analyze this experiment.

In the present work we study an alternative approach to the near-field optical characterization of photonic crystals. We suggest exciting the crystal with an incident laser beam. This may be idealized as an excitation by a δ function in momentum space. We use NSOM in the transmission mode to measure directly the local electromagnetic mode structure on the surface of a photonic crystal in coordinate space. The NSOM images are Fourier analyzed in order to extract information on the band-gap structure and refractive index distribution in the photonic crystal. We show this approach to be straightforward and simple.

We also apply our technique to the study of a two-dimensional ''plasmonic crystal'': a gold-coated rectangular bigrating, which possesses properties similar to the properties of a photonic crystal. Far-field optical properties of similar plasmonic crystals have been studied very recently[6] but no near-field studies of such crystals have been reported to date.

The surface plasmon (SP) is a fundamental electromagnetic excitation mode of a metal-dielectric interface.[7] The SP is free to propagate along the metal surface, but its field decays exponentially in both media in the direction perpendicular to the interface. Thus the spatial distribution of the SP field is inaccessible to far-field optical techniques. The development of NSOM has created ways to probe the SP field directly. SP propagation along the interface has been imaged in Ref. 8. SP scattering by *in situ* created individual surface defects has been studied and some prototype two-dimensional optical elements able to control SP propagation have been demonstrated.[9,10]

A periodic array of defects in the metal-dielectric interface should exhibit the properties of a two-dimensional ''plasmonic crystal'' when the periodicity of the structure is comparable with the wavelength of the SP. A complicated system of band gaps has indeed been measured in Ref. 6 using different bigratings. In the present paper we report our measurements of the local electromagnetic mode structure of a plasmonic crystal and derive some parameters of SP interaction with defects that constitute the bigrating. We present a

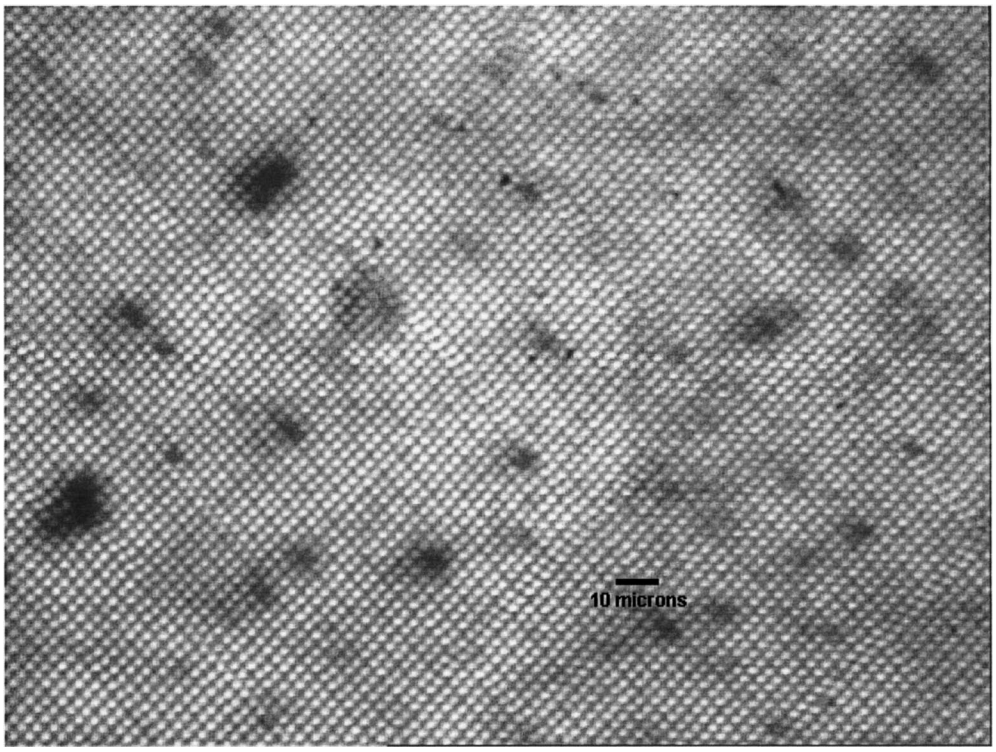

FIG. 1. Far-field transmission image of the photonic crystal structure taken with an optical microscope using bottom face illumination with white light.

similar description of the results obtained with two-dimensional photonic and plasmonic crystals.

EXPERIMENTAL SETUP AND SAMPLES

We have studied two different kinds of photonic band-gap structures. The first sample studied is similar to the photonic crystal used in Ref. 5. It is a fiber bundle obtained from Schott Glass Technologies, Inc. made of two glasses with similar indices of refraction. The bundle is a two-dimensional rectangular lattice of glass with a higher refractive index embedded in a matrix glass with a lower refractive index. The period of the structure is approximately 3 μm. Figure 1 shows an image of a top face of the sample taken with a conventional optical microscope using bottom face illumination with a white light source. The image shows good periodicity of the structure although some dislocations and blemishes are present. Both faces of the sample are polished. The thickness of the sample is about 100 mm.

The second sample is a gold-coated two-dimensional rectangular calibration grating with a period of about 1 μm obtained from Digital Instruments, Inc. An atomic force microscope image of the sample surface is shown in Fig. 2. According to the manufacturer, a 30-nm layer of gold has been deposited by thermal evaporation on top of a glass grating coated with 800 nm of aluminum and 4 nm of chromium. In the absence of grooves such a ''sandwich'' structure supports surface plasmon propagation with a spectrum close to the spectrum of SPs on the surface of an infinitely thick flat gold sample. (The decay length of the SP field inside gold is about $l=\lambda/2\pi\epsilon_{\mathrm{Au}}^{1/2}$.[7] At a wavelength of 633 nm this gives $l=36$ nm.) The grooves scatter the SP field in the plane of propagation. Also they couple the SP field to photons in free space. Since the period of the structure is comparable with the wavelength of plasmons: $\lambda_p=\lambda[(\epsilon_{\mathrm{Au}}+1)/\epsilon_{\mathrm{Au}}]^{1/2}=590$ nm, where $\lambda=633$ nm is the wavelength of light in air, this sample must behave as a ''plasmonic crystal.'' There should be forbidden gaps in the SP momentum space. The spatial topology of such SP forbidden gaps in a similar rectangular bigrating has been studied in Ref. 6.

Our NSOM setup is described in detail in Ref. 10. It allows us to measure simultaneously surface topography using optical shear-force feedback,[4] and the spatial distribution of the optical signal in near-field proximity to the sample surface. In order to study the samples described, our experimental setup has been modified as follows [Figs. 3(a) and 3(b)]. The photonic crystal from Fig. 1 has been studied using NSOM working in a transmission mode as shown in Fig.

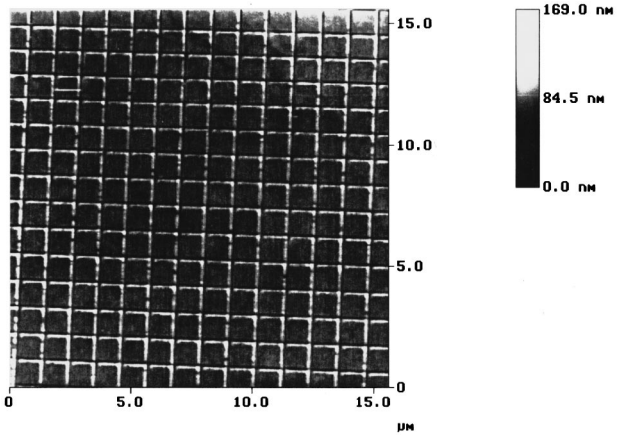

FIG. 2. Atomic force microscopic image of the plasmonic crystal surface topography.

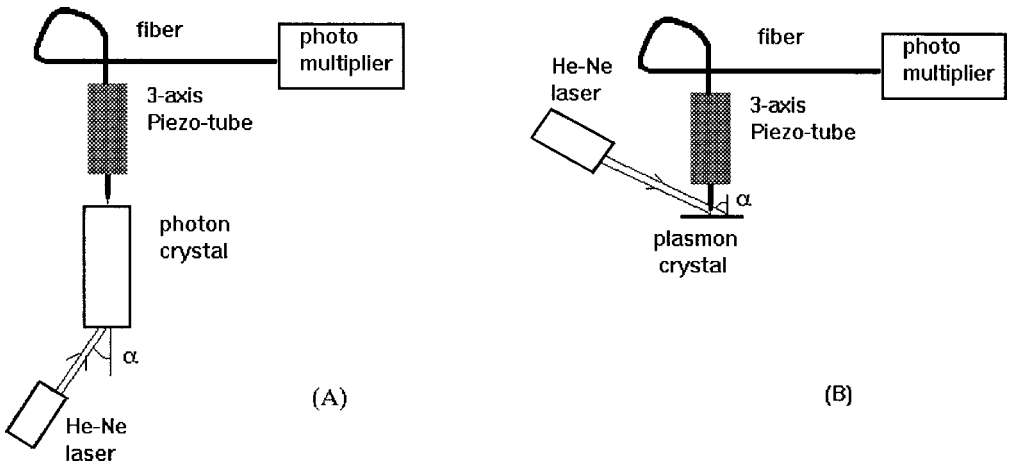

FIG. 3. Experimental setups for studying optical properties of (a) the photonic crystal and (b) the plasmonic crystal.

3(a). The angle of the bottom face illumination was varied and the field distribution on the top face was studied as a function of this angle.

The SPs on the surface of the plasmonic crystal from Fig. 2 were excited in reflection [Fig. 3(b)]. It is impossible to excite a SP wave on the flat gold-air interface by illumination of the surface from air. At a given frequency the momentum of photons in air is smaller than the momentum of plasmons. The presence of the periodically spaced grooves leads to a modification of the momentum conservation law: integer multiples of the reciprocal lattice vectors of the bigrating can be added to the photon and plasmon momenta. This leads to the possibility of SP excitation by photons illuminating the bigrating at certain resonant angles. Accordingly, the angle of sample illumination was varied in the experimental geometry shown in Fig. 3(b) in order to achieve SP excitation. *P*-polarized light from a He-Ne laser has been used. The SP field distribution has been measured using an uncoated tapered fiber tip in our NSOM. Although the resolution of a NSOM is higher when metal-coated tips are used,[4] an uncoated fiber tip introduces a much smaller perturbation in the SP field distribution.[10] This results from the much smaller difference between the dielectric constants of the glass tip and air ($\epsilon_{\text{tip}}-1$) in comparison with the difference between the dielectric constants of air and metal.

PHOTONIC CRYSTAL IMAGING

Near-field optical images of the photonic crystal sample obtained at different angles of excitation are shown in Figs. 4(a)–4(c). The topographical images taken simultaneously show no features higher than 10 nm and do not correlate with the optical ones. The optical images in Fig. 4 exhibit general periodicity of the refractive index structure (a 3-μm period in both directions). Some distortions in the images may be attributed to the dislocations observed in Fig. 1.

The main feature of these images is an appearance of additional periodicity and a richer spatial frequency spectrum at larger excitation angles. This feature is quite clear from the Fourier spectra presented in Figs. 5(a) and 5(b). Such behavior is easy to understand when the general theory of a photonic band-gap material is applied to our particular case (an extensive theoretical description of two-dimensional photonic crystals can be found in Ref. 11).

When a monochromatic electromagnetic wave of frequency ω propagates in a dielectric medium with a periodic dielectric constant $\epsilon(\mathbf{r})=\epsilon_0+\epsilon_1(\mathbf{r})$ (ϵ_0 is an average dielectric constant of a medium), the classical wave equation may be written in a form resembling the Schrödinger equation:

$$-\nabla^2\mathbf{E}+\vec{\nabla}(\vec{\nabla}\mathbf{E})-\omega^2\epsilon_1(\mathbf{r})\mathbf{E}/c^2=\epsilon_0\omega^2\mathbf{E}/c^2. \qquad (1)$$

In this equation $\epsilon_1(\mathbf{r})$ plays a role analogous to the periodic potential $U(\mathbf{r})$ in the Schrödinger equation for an electron in a crystal. In the two-dimensional crystal under consideration the photon motion may be decomposed into the motion in a periodic potential (perpendicular to the fiber bundle axis) and the free motion along the structure with momenta $k_\perp$ and $k_\parallel$, so that $k_\parallel^2+k_\perp^2=\epsilon_0\omega^2/c^2$. Thus larger excitation angles correspond to a larger momentum of motion in a periodic potential. Consequently, higher harmonics may be expected in the near-field image. To some extent our data are similar to the images of metal or semiconductor crystals obtained in scanning tunneling microscopy with different tunneling voltages applied. In both cases one can vary the particle (electron or photon) energy in the periodic potential as a free parameter.

The intensities of different spectral peaks in Fig. 5 contain information about the periodic part of the dielectric constant $\epsilon_1(\mathbf{r})$ of the photonic crystal. The Bloch theorem can be used in order to extract this information. Exact theory[11] gives slightly different equations for different polarization states of the electromagnetic field in the two-dimensional photonic crystal. On the other hand, regular individual optical fibers (not polarization maintaining ones) similar in design to the fibers that constitute our photonic crystal (Fig. 1) scramble the polarization of incoming light. Generally, NSOM fiber tips also do not preserve the polarization of the light,[12] so we can disregard this difference and consider the field to be scalar. In this case, the wave equation looks exactly like the Schrödinger equation for an electron in a periodic potential $U=\omega^2\epsilon_1/c^2$ and we can directly use the standard representation of the Schrödinger equation in momentum space[13]:

$$(k_\parallel^2+k_\perp^2-\epsilon_0\omega^2/c^2)A_{\mathbf{k}_\perp}+\sum_{\mathbf{G}} U_{\mathbf{G}}A_{\mathbf{k}_\perp-\mathbf{G}}=0, \qquad (2)$$

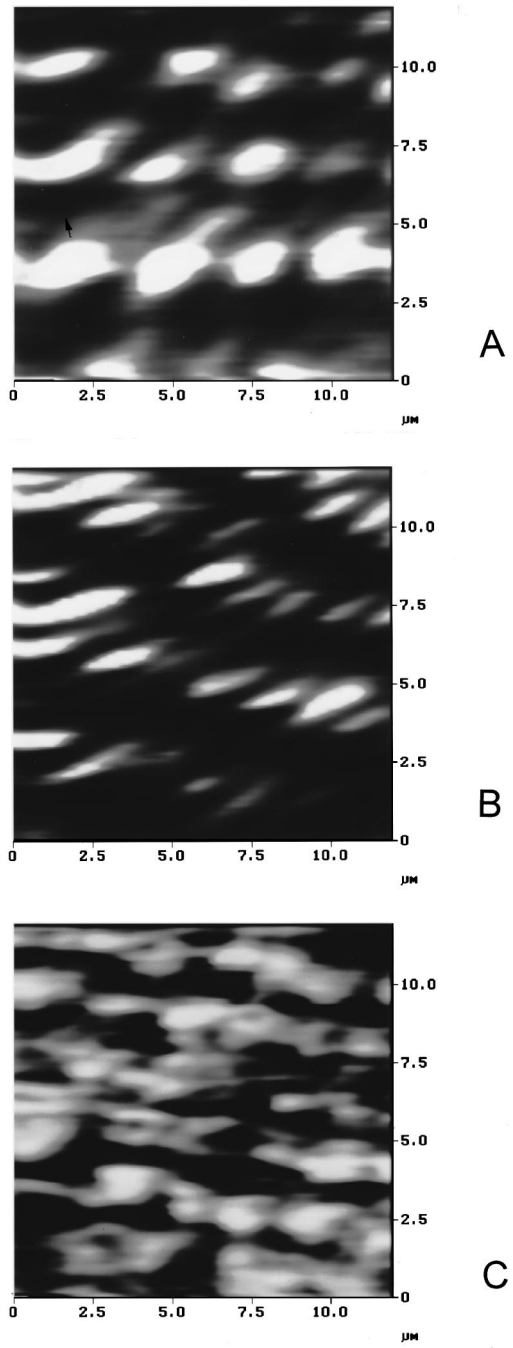

FIG. 4. Transmission near-field optical images of the photonic crystal taken at different angles of bottom face illumination: (a) 0°, (b) 7°, (c) 15°.

where $U(\mathbf{r})=\Sigma_{\mathbf{G}}U_{\mathbf{G}}e^{i\mathbf{G}\cdot\mathbf{r}}$ is the periodic potential, $\mathbf{G}$ are the reciprocal lattice vectors, and

$$E=e^{i\mathbf{k}_{\perp}\mathbf{r}}\sum_{\mathbf{G}} A_{\mathbf{k}_{\perp}-\mathbf{G}}e^{-i\mathbf{G}\cdot\mathbf{r}} \tag{3}$$

is the Bloch wave solution of the equation.

Usually it is reasonable to assume that the coefficients $A_{\mathbf{k}}$ are very small for large absolute values of $\mathbf{k}$. We also see this from our experimental measurements in Fig. 5. This reduces the Schrödinger equation (2) to a small number of linear equations relating $A_{\mathbf{k}}$ and $U_{\mathbf{G}}$.

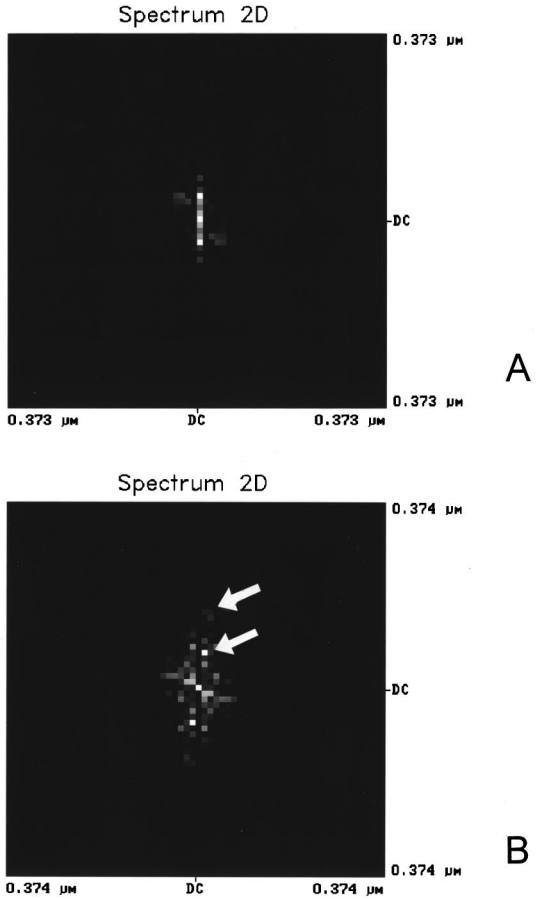

FIG. 5. Images (a) and (b) are the Fourier spectra of the images from Figs. 4(a) and 4(b), respectively. Additional periodicity and a richer spatial frequency spectrum appear at larger excitation angles. Spectral peaks near the first- and second-order reciprocal lattice vectors are shown by arrows in (b).

We have performed a one-dimensional reconstruction of the photonic crystal refractive index as follows. The physical value measured in the experiment is the local electromagnetic field intensity on the face of the photonic crystal. If a one-dimensional Bloch wave propagates in the crystal along the x direction, its field distribution can be written as $E=\Sigma_n A_n e^{i(kx-\omega t)}e^{i2\pi nx/a}$, where a is the period of the crystal in the direction of propagation and n is an integer. An averaged field intensity is equal to

$$I=1/2\sum_{mn} A_m A_n \cos[2\pi(n-m)x/a]. \tag{4}$$

Thus measurements of the intensities of spectral peaks at $2\pi n/a$ in Fig. 5 allow us to recover the coefficients A_n of the Bloch wave. The first three coefficients have been measured. Substitution of these A_n in Eq. (2) allows us to obtain three coefficients U_n of the Fourier spectrum of the crystal potential in this direction: $U(x)=\Sigma_n U_n e^{i2\pi nx/a}$. The results of our measurements are represented in Fig. 6, which shows variations of the refractive index of the photonic crystal along one direction. The amplitude of these variations agrees well with the indices of the bulk unprocessed glasses used to make the crystal, which were measured by Schott Glass Technologies, Inc. at 590 nm to be 1.657 and 1.676. Thus the simple ap-

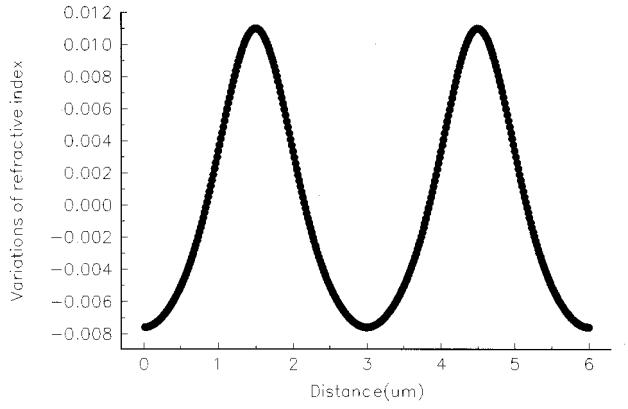

FIG. 6. Reconstructed refractive index variations in the photonic crystal along one direction.

proach introduced above allows a reasonable description of the photonic crystal properties.

PLASMONIC CRYSTAL STUDY

A surface plasmon can be excited on the surface of the rectangular bigrating (Fig. 2) at a number of resonant angles. These angles α_n are determined by the quasimomentum conservation law: $k \sin \alpha_n = k_p + 2\pi n/a$, where k_p is the SP wave vector on the flat metal surface, a is the period of the structure in the direction of propagation, and n is an integer. The angular dependence of the optical signal measured at the output of the fiber tip of our NSOM near one of the resonant angles is shown in Fig. 7. Resonant excitation of SP has been clearly detected. The angular width of the resonant curve is narrower than in Ref. 6. This may be attributed to the better surface quality of the bigrating used in our experiments.

We simultaneously measured topography of the sample and the optical field distribution with resonant SP excitation. Some examples of these images are shown in Figs. 8(a)–8(c). The periodicity properties of the optical images are much more complicated than those of a topographical image. This is evident from the Fourier image of Fig. 8(c) shown in Fig. 9. The brightest spectral peak in this image corresponds to a spatial period of 3.5 μm. Our calculations show this value to be approximately equal to half of the largest effective wavelength of SP propagating along the surface of the plasmonic crystal: $\lambda_p^* = 2\pi/k_p^* = 2\pi/(k_p + 2\pi n/a) = 7.26$ μm at $n = -2$. This indicates that we observe interference pattern of the plasmon Bloch waves in the image in Fig. 8(c). Complicated interference patterns formed by SPs on the flat gold surface had been observed in Ref. 14. They were attributed to the presence of surface defects. The surface quality of our plasmonic crystal structure is very good (Fig. 2), nevertheless some surface defects can be seen. So the appearance of SP Bloch wave interference patterns in the images is natural.

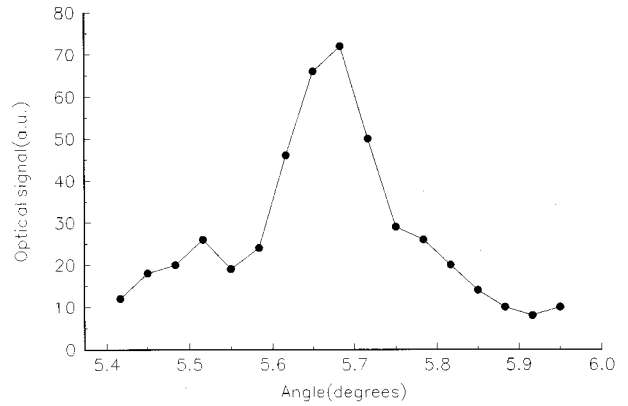

FIG. 7. Angular dependence of the NSOM optical signal near one of the SP resonances.

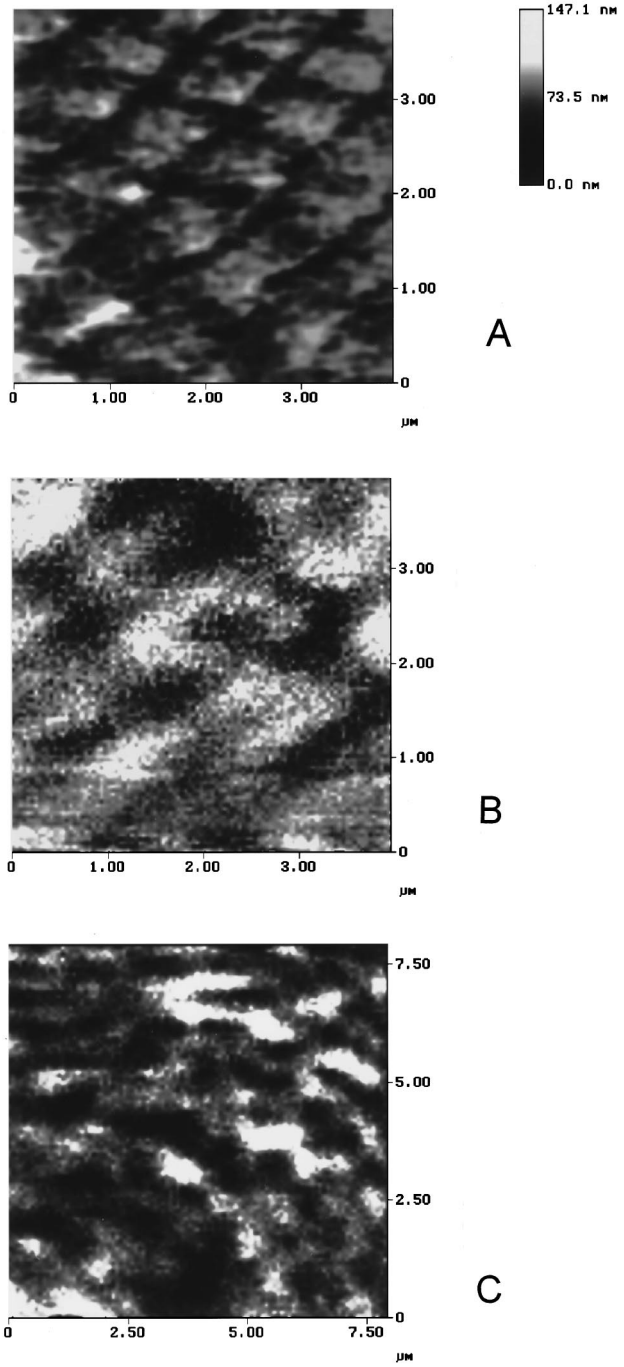

FIG. 8. Topography (a) and optical near-field distributions in the plasmon crystal measured on different scales (b), (c) with surface plasmon excitation.

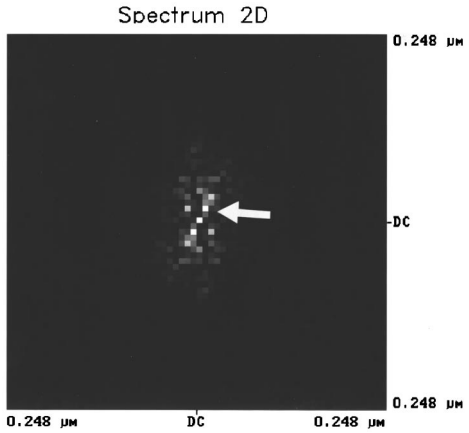

FIG. 9. Fourier spectrum of the image in Fig. 8(b). The spectral peak at a spatial period of 3.5 μm is shown by an arrow.

NSOM allows us to modify a surface under investigation. Direct-write lithography may be performed by coupling UV light into a fiber tip[9] or by delicate mechanical touching of the sample surface.[15] Mechanical surface modification is especially easy in the case of a soft sample such as a gold surface. We have verified experimentally that artificially created defects lead to the appearance of very pronounced long-period interference patterns in the vicinity of defects. The results of such an experiment are shown in Fig. 10. A defect has been created in the middle of the NSOM field of view on top of the periodic plasmon crystal structure, which has also been slightly modified. A shadowlike phenomenon is seen just behind the defect (the direction of SP propagation is shown by an arrow). A set of stripes with a period on the order of 3 μm has become very pronounced. These results indicate that we are indeed dealing with the interference of SP Bloch waves.

The SP field distribution and band-gap structure of a plasmonic crystal can be calculated analytically in the limit of small roughness if the surface topography is known.[16] In our case the surface roughness cannot be considered to be small since the depth of the grooves in Fig. 2 is comparable with the thickness of the gold film. Rather complicated numerical calculations are required to compare the results of our measurements with an exact theory also presented in Ref. 16. Such a comparison is desirable and could give a good test of the electrodynamics of metals on a submicrometer scale.

A simpler approach is to use the concept of effective plasmon refractive index introduced in Ref. 10. SP phase velocity depends on the metal film thickness. The effective refractive index of a surface defect may be introduced as a ratio of SP phase velocities on the defect and on the background metal film area. Use of this concept makes the description of photonic and plasmonic crystals similar. Effective SP refractive index distribution over the crystal surface may be derived using the procedure described above for the case of a photonic crystal. Unfortunately, SP Bloch wave interference makes the situation more complicated since they contribute substantially to the Fourier spectrum of the SP field distribution and the amplitude of the reflected waves is generally unknown. Only an order of magnitude estimate of the effective refractive index can be derived from Fig. 9. It follows from Eq. (2) that $\omega^2\epsilon_1/c^2 \sim (2\pi/a)^2 A_{n+1}/A_n$. This leads to $\Delta n \sim (\lambda/a)^2 A_{n+1}/A_n \sim 0.05$ as an estimate of the amplitude of the effective SP refractive index variations. This number is in general agreement with the values of SP refractive indices of different surface defects derived in Ref. 10.

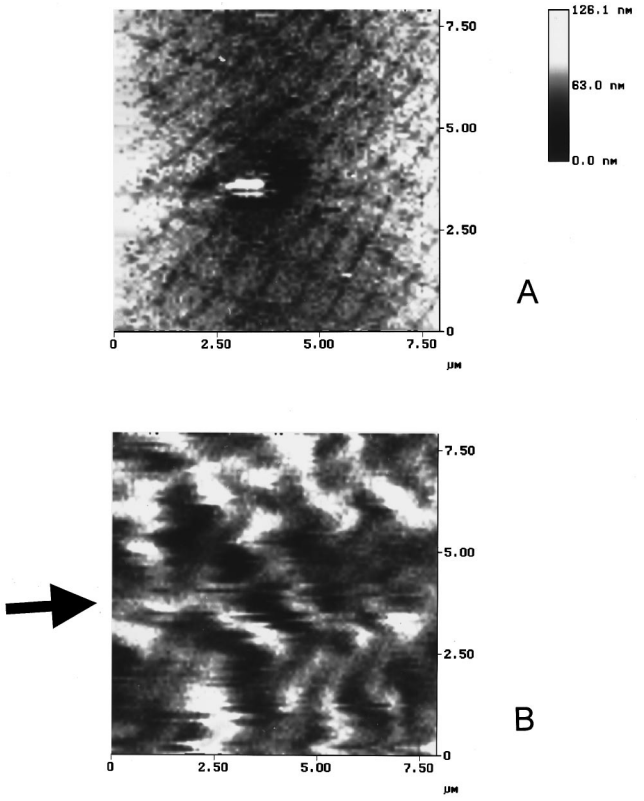

FIG. 10. Topography (a) and optical near-field distribution (b) around artificially created defect on the surface of the plasmon crystal structure. The direction of SP propagation is shown by an arrow.

CONCLUSION

The main results of this paper may be summarized as follows.

An alternative method for studying photonic crystals using NSOM has been introduced. In a previous study [5] the photonic crystals were excited by light from a NSOM tip. This may be idealized as an excitation with a δ function in coordinate space. The transmitted light distribution was analyzed as a function of the absolute value of its momentum.

In the present work photonic crystals were excited with an incident laser beam. This may be idealized as an excitation by a δ function in momentum space. NSOM images are Fourier analyzed in order to extract information on refractive index distributions in the photonic crystals.

Interference patterns produced by SP Bloch waves in the plasmonic crystal have been directly observed.

[1] J. D. Joannopoulos, R. D. Meade, and J. N. Winn, *Photonic Crystals* (Princeton University Press, Princeton, NJ, 1995).

[2] E. Yablonovitch, Phys. Rev. Lett. **58**, 2059 (1987); W. M. Robertson, G. Arjavalingam, R. D. Meade, K. D. Brommer, A. M. Rappe, and J. D. Joannopoulos, *ibid.* **68**, 2023 (1992).

[3] K. Inoue, M. Wada, K. Sakoda, M. Hayashi, T. Fukushima, and A. Yamanaka, Phys. Rev. B **53**, 1010 (1996); A. Rosenberg, R. J. Tonucci, H. B. Lin, and A. J. Campillo, Opt. Lett. **21**, 830 (1996); H. B. Lin, R. J. Tonucci, and A. J. Campillo, Appl. Phys. Lett. **68**, 2927 (1996).

[4] *Near Field Optics*, edited by D. W. Pohl and D. Courjon (Kluwer, Dordrecht, 1993).

[5] E. B. McDaniel, J. W. P. Hsu, L. S. Goldner, R. J. Tonucci, E. L. Shirley, and G. W. Bryant, Phys. Rev. B **55**, 10 878 (1997).

[6] R. A. Watts, J. B. Harris, A. P. Hibbins, T. W. Preist, and J. R. Sambles, J. Mod. Opt. **43**, 1351 (1996).

[7] H. Raether, *Surface Plasmons*, Springer Tracts in Modern Physics Vol. 111 (Springer, Berlin, 1988).

[8] P. Dawson, F. de Fornel, and J.-P. Goudonnet, Phys. Rev. Lett. **72**, 2927 (1994).

[9] I. I. Smolyaninov, D. L. Mazzoni, and C. C. Davis, Phys. Rev. Lett. **77**, 3877 (1996).

[10] I. I. Smolyaninov, D. L. Mazzoni, J. Mait, and C. C. Davis, Phys. Rev. B **56**, 1601 (1997).

[11] A. A. Maradudin and A. R. McGurn, in *Photonic Band Gaps and Localization*, edited by C. M. Soukoulis (Plenum, New York, 1993), p. 247.

[12] J. K. Trautman, E. Betzig, J. S. Weiner, D. J. DiGiovanni, T. D. Harris, F. Hellman, and E. M. Gyorgy, J. Appl. Phys. **71**, 4659 (1992).

[13] C. Kittel, *Introduction to Solid State Physics* (Wiley, New York, 1976).

[14] S. I. Bozhevolnyi, I. I. Smolyaninov, and A. V. Zayats, Phys. Rev. B **51**, 17 916 (1995).

[15] S. I. Bozhevolnyi and F. A. Pudonin, Phys. Rev. Lett. **78**, 2823 (1997).

[16] A. A. Maradudin, in *Surface Polaritons*, edited by V. M. Agranovich and D. L. Mills (North-Holland, Amsterdam, 1982), p. 405.